Spatial characterization of the plasma density in a magnetically expanding plasma using permanent magnets

Tomoyo SASAKI, Kazunori TAKAHASHI, Kaoru OGUNI, and Tamiya FUJIWARA
Department of Electrical and Electronic Engineering, Iwate University, Morioka, Iwate 020-8551, Japan

(Received: 31 August 2008 / Accepted: 14 November 2008)

It is demonstrated that a spatial characterization of a plasma density in a magnetically expanding plasma using multi-pole permanent magnets (PMs), which contains an electric double layer generating a supersonic ion beam. The machine has a glass tube (source tube) surrounded by PMs for plasma production and a grounded diffusion chamber. In the source tube, the azimuthal profile of the ion saturation current is non-uniform due to the multi-pole magnetic fields and has several peaks correlating with the magnetic-field configuration. On the other hand, the result in the diffusion chamber shows a radially parabolic and azimuthally uniform profile. Thus, it is considered that there is no influence of the multi-pole fields on the density profile in the diffusion chamber unlike the source tube.

Keywords: expanding plasma, inductively coupled plasma, permanent magnets, multi-pole magnetic field, plasma structure

1. Introduction

It is well known that a nonlinear plasma-potential structure which can generate a supersonic ion beam is formed in expanding plasmas; the process is expected to be utilized for applications in many research fields such as space physics [1,2], plasma thrusters [3-5], and so on. The recent works in the expanding helicon plasmas show that the magnetic-field configuration is the critical parameter for the formation of an electric double layer (DL) in the expanding plasmas [6,7]. Charles and Boswell have suggested that the new type electric thruster, named the helicon double layer thruster, can yield a long-lifetime because it does not require any electrodes for ion extraction [8-11].

In previously reported experiments on magnetically expanding plasmas containing the DLs, electromagnets are used to generate the steady-state magnetic fields [3-11]. In recent years, a compact helicon source introducing permanent magnets (PMs) for the DL and ion beam formations are studied by Shamrai *et al*. [12], which can reduce the consumed electricity in the system. They reported that the cusp fields created by PMs prevent the plasma diffusion, the DL formation, and the ion beam generation; the magnetic fields created by the electromagnets are superimposed in their experiments. After that, Takahashi *et al*. have achieved the DL and the ion beam formations in a solenoid-free expanding plasma using only the PMs [13], where double concentric PMs arrays are employed in order to create the constant fields area for the plasma production and the expanding field for the formation of the DL. It is considered that this source is useful for the development of more efficient and compact plasma thruster; it is important to understand the basic behavior of the source from the viewpoints of the applications. Generally, spatial profiles of the plasma parameters would be influenced by the magnetic-field and the antenna configurations in magnetized rf plasmas [14-16].

In the present paper, we report two-dimensional profiles of the plasma density in the previously reported solenoid-free plasma using the PMs, which contains the DL [13].

2. Experimental setup

The experimental setup is schematically shown in Fig. 1. The machine has a 30-cm-long and 26-cm-diam grounded diffusion chamber connected with a 20-cm-long and 6.6-cm-diam pyrex glass tube (source tube), where $z = 0$ is defined as the boundary between the source tube and the diffusion chamber. Here, *x, y,* and

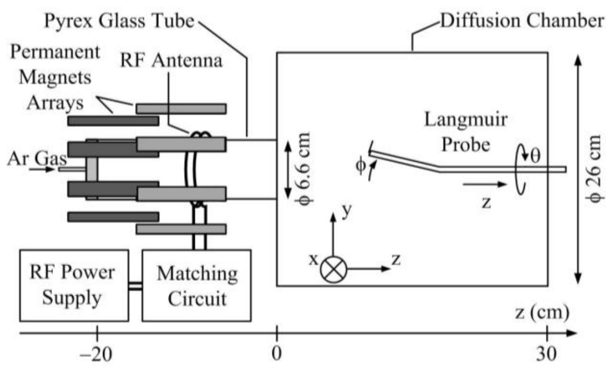

Fig. 1 Schematic diagram of experimental setup.

author's e-mail: t3308009@iwate-u.ac.jp

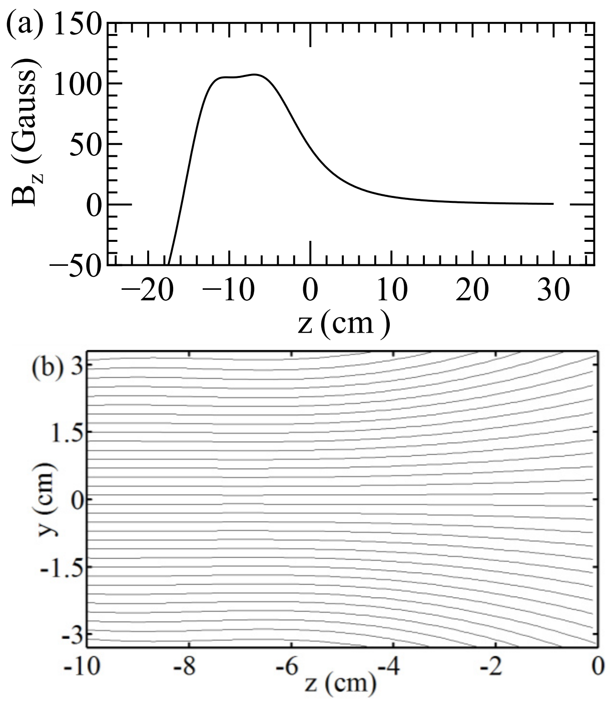

Fig. 2 (a) Axial profile of the calculated axial component B_z of the magnetic-field strength produced by the PMs arrays presented at the left of Fig. 1. (b) *z*-*y* profile of the field-line structures in the source tube.

z axes are defined as indicated in Fig. 1. The chamber is evacuated to a base pressure 2×10^{-6} Torr by a diffusion/rotary pumping system, and the argon gas is introduced from the source side through a mass flow controller. The working gas pressure is kept at 0.4 mTorr in the present experiment. An inductively coupled rf plasma is excited by a double-turn loop antenna surrounding the source tube ($z = -10$ cm) and powered from an rf generator of frequency 13.56 MHz and power 250 W through a matching circuit.

Double concentric arrays consisting of sixteen Neodymium Iron Boron (NdFeB) magnets (10 cm in length, 1.5 cm in width, and 0.5 cm in thickness) are mounted around the source tube in order to generate the axially constant magnetic field near the antenna for the plasma production and the axially expanding magnetic field for the DL formation. The side and front views of the magnets are presented in Figs. 1 and 3, respectively. The axial profile of the axial component B_z of the local magnetic-field strength is calculated by the magnetic-moment method, where we have confirmed that the result is in good agreement with the measured one as previously reported in Ref. [13]. In addition, the *z*-*y* profile of the field-line structures in the source tube is shown in Fig. 2(b). The constant field of about one hundred Gauss is generated over 7 cm (-13 cm $< z < -6$ cm) and the field is expanding near the outlet of the source tube into a few Gauss. We have also confirmed that the DL is generated at the diverging-field area (z = -3 – 1 cm) [13]. The calculated *x*-*y* profiles of the magnetic-field strength $B_\perp$ in the direction perpendicular to *z*-axis at $z = -7$ cm and $z = -5$ cm in the source tube are shown in Figs. 3(a) and 3(b), respectively, as contour plot in gray scale, where all of the PMs have radially inward magnetization. The solid arrows in Fig. 3 indicate the local magnetic-fields vector in *x*-*y* plane and the inner wall of the glass tube is drawn as a 6.6-cm-diam white circles. It is confirmed in Figs. 3(a) and 3(b) that the multi-pole magnetic fields are generated in the source tube. At $z = -7$ cm axially inside the PMs arrays, radially inward magnetic fields $B_\perp$ are generated at the azimuthal positions of each PM near the glass wall ($r \sim 3$ cm). At $z = -5$ cm axially downstream of the PMs arrays, on the other hand, radially outward magnetic fields $B_\perp$ are generated at the azimuthal positions between PMs, where the axially diverging magnetic fields is formed. In this experiment, the complicated magnetic-field structure would play an important role in charged-particle behaviors.

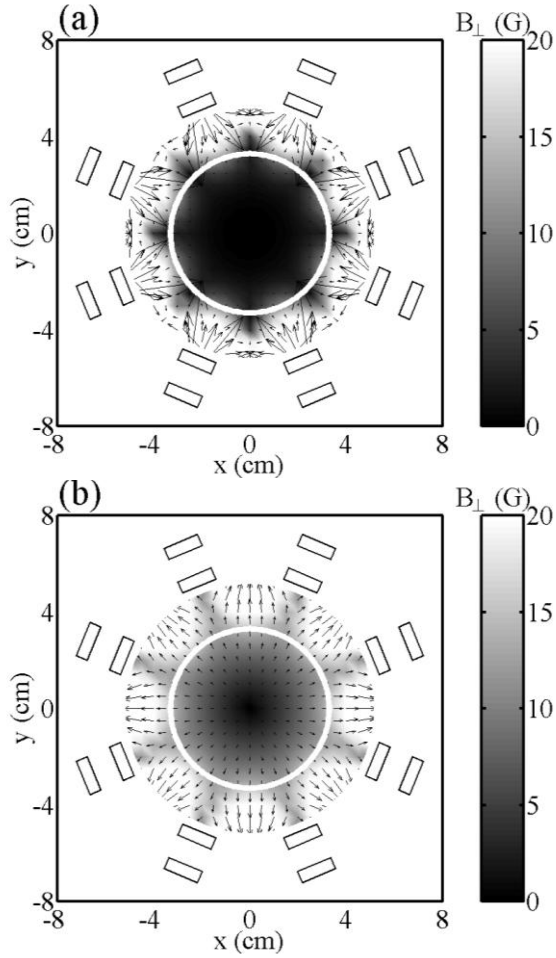

Fig. 3 The calculated *x*-*y* profiles of the magnetic-field strength $B_\perp$ in the direction perpendicular to *z*-axis at (a) $z = -7$ cm and (b) $z = -5$ cm in the source tube (contour plot), where the white circles and open rectangles show the glass wall and PMs having radially inward magnetization, respectively. The solid arrows indicate the local magnetic-field vector in the perpendicular direction.

A conventional cylindrical Langmuir probe (LP) combined with a three-dimensionally movable probe-system, which can yield *x-y* profiles of the plasma parameters, is inserted from the downstream side of the diffusion chamber. In the system, three-dimensional measurements can be done by changing two angles ϕ and θ as presented in Fig. 1.

3. Experimental results and discussion

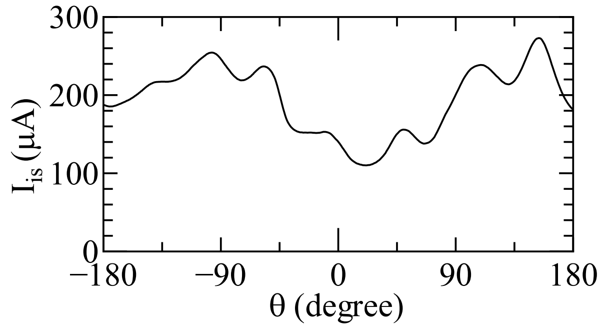

Fig. 4 Azimuthal profile of the ion saturation current I_{is} of the LP at $z = -7$ cm and $r = 2.6$ cm in the source tube, where the LP is biased at −60 V to collect ions and $\theta = 0$ is defined as the left side in Fig. 5-6.

Figure 4 shows azimuthal profile of the ion saturation current I_{is} of the LP at $z = -7$ cm and $r = 2.6$ cm in the source tube, where the local plasma potential at the center of the source tube is about 60 V as reported in Ref. [13] and the LP is negatively biased at −60 V. Thus, the negative bias applied to the LP is considered to be enough to correct the ion saturation current, which is a function of the plasma density, electron temperature, and ion temperature. The measured electron temperature in the diffusion chamber is about 8 eV, but we have no information of the temperatures of the electrons in the source tube and ions. Therefore, the ion saturation current can not exactly show the plasma density but can be an indicator of the plasma density. In Fig. 4, $\theta = 0$ is defined as the left side in Fig. 5-6. By measuring the azimuthal profile of I_{is} at each radial position r with about 0.3 cm interval, viewgraphs of *x-y* profile of the ion saturation current I_{is} as shown in Figs. 5(a) and 5(b) can be obtained, where Figs. 5(a) and 5(b) are the result at $z = -7$ cm and $z = -5$ cm, respectively. It is found that the density profiles at $z = -7$ cm and $z = -5$ cm are non-uniform in the azimuthal direction, especially near the wall of the glass tube. It is noticed that the plasma density appears to be high at the azimuthal position where the PMs are absent, that is, troidal angle $\theta = 45 \times n$ degree (n is an integer from 0 to 8). In addition, the density gradient at $z = -5$ cm shown in Fig. 5(b) seems to be larger than that at $z = -7$ cm shown in Fig. 5(a). Comparing the positions of $\theta = 45 \times n$ and the magnetic-field structures shown in Fig. 3(a), there corresponds to the azimuthal positions where the perpendicular magnetic fields have a radially inward

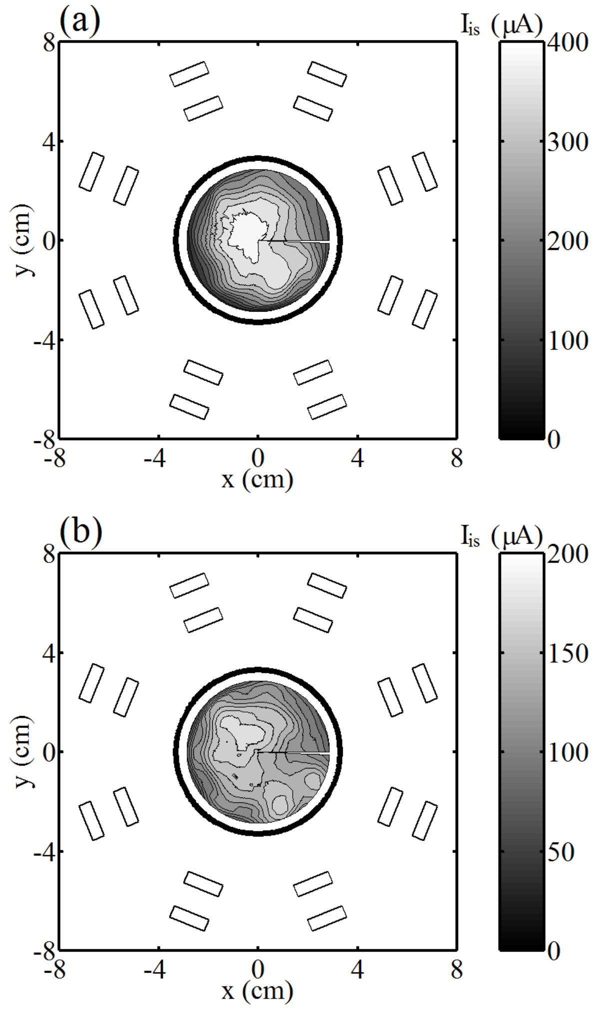

Fig. 5 *x-y* profiles of the ion saturation current I_{is} of the LP at (a) $z = -7$ cm and (b) $z = -5$ cm in the source tube, where the bold lines and open rectangles show the glass wall and PMs having radially inward magnetization, respectively.

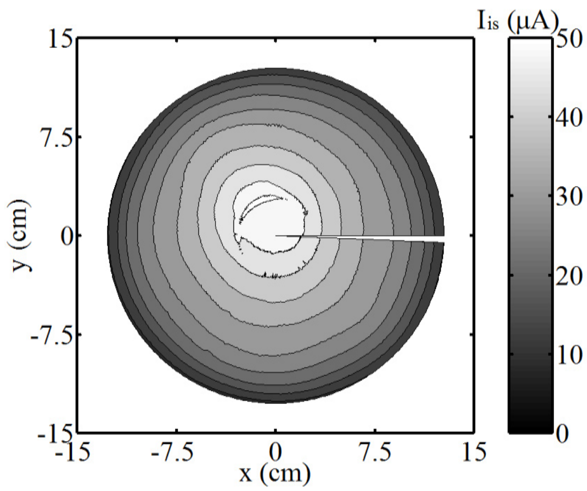

Fig. 6 *x-y* profiles of the ion saturation current I_{is} of the LP at $z = 10$ cm in the diffusion chamber.

direction at $z = -7$ cm. That is to say, inside the PMs arrays at $z = -7$ cm, the magnetic-field lines are converging at these azimuthal positions near the PMs. Downstream of the PMs arrays at $z = -5$ cm, on the other hand, the perpendicular magnetic fields at the above-mentioned azimuthal positions have a radially outward direction; it is found that the magnetic-field lines at the azimuhtal positions where the PMs are absent are more divergent than those near the PMs. Therefore, the plasma produced by the rf antenna at $z = -10$ cm is slightly compressed by the converging fields near $z = -7$ cm at the azimuthal positons where the PMs are set; it can cause the decrease in the density near the PMs. After that, the plasma can flow along the magnetic-field lines diverging at the positions where the PMs are absent. Hence, the density gradient near the wall at $z = -5$ cm is considered to be more conspicuous than that at $z = -7$ cm. In addition, it should be noticed in Fig. 5 that the left-side ($x < 0$) plasma density is higher than the right-side one in the source tube, which is originating from the configuration that rf power is fed from the left side.

The two dimensional characterization of the plasma density in the diffusion chamber downstream of the DL is also investigated. Figure 6 shows the *x-y* profile of the ion saturation current I_{is} at $z = 10$ cm, where the magnetic-field strength B_z is below ten Gauss. It is found that the profile is radially parabolic and azimuthally uniform, hence it is found the multi-pole fields created by the PMs does not affect the density profile in the diffusion area downstream of the DL.

4. Conclusion

The spatial profiles of the plasma density are experimentally investigated by the three-dimensionally movable Langmuir probe system in the magnetically expanding plasma using permanent magnets arrays, which contains the DL causing the ion acceleration. The diverging magnetic-field configuration for the DL formation and the ion acceleration can be created by employing the double concentric arrays of the PMs, where the magnetic-field structures are confirmed to be multi-pole. Near the glass wall in the source tube, it is experimentally found that the density profile is azimuthally and radially non-uniform due to the multi-pole fields and the rf-antenna configuration, respectively. In the diffusion chamber downstream of the DL, on the other hand, the density profile in the diffusion chamber is radially parabolic and azimuthally uniform. Our results show that the multi-pole fields affect the density profile only in the source tube.

5. Acknowledgements

This work was supported by Grant-in-Aid for Young Scientists (B, 20740317) from the Ministry of Education, Culture, Sports, Science and Technology, Japan. This work is also partially supported by TEPCO Research Foundation.

[1] G. Hairapetian and R. L. Stenzel, Phys. Rev. Lett. **61**, 1607 (1988).

[2] R. E. Ergun, Y.-J. Su, L. Andersson, C. W. Carlson, J. P. McFadden, F. S. Mozer, D. L. Newman, M. V. Goldman, and R. J. Strangeway, Phys. Rev. Lett. **87**, 045003 (2001).

[3] S. A. Cohen, N. S. Siefert, S. Stange, R. F. Boivin, E. E. Scime, and F. M. Levinton, Phys. Plasmas **10**, 2593 (2003).

[4] C. Charles and R. W. Boswell, Appl. Phys. Lett. **82**, 1356 (2003).

[5] X. Sun, S. A. Cohen, E. E. Scime, and M. Miah, Phys. Plasmas **12**, 103509 (2005).

[6] C. Charles and R. W. Boswell, Appl. Phys. Lett. **91**, 201505 (2007).

[7] I. A. Biloiu, E. E. Scime, and C. Biloiu, Appl. Phys. Lett. **92**, 191502 (2008).

[8] C. Charles and R. W. Boswell, Phys. Plasmas **11**, 1706 (2004).

[9] O. Sutherland, C. Charles, N. Plihon, and R. W. Boswell, Phys. Rev. Lett. **95**, 205002 (2005).

[10] C. Charles, R. W. Boswell, and M. A. Lieberman, Appl. Phys. Lett. **89**, 261503 (2006).

[11] K. Takahashi, C. Charles, R.W. Boswell, T. Kaneko, and R. Hatakeyama, Phys. Plasams **14**, 114503 (2007).

[12] K. P. Shamrai, Y. V. Virko, V. F. Virko, and A. I. Yakimenko, Proceedings of the 42nd AIAA/ASME/SAE/ASEE Joint Propulsion Conference and Exhibit, California 2006, (the American Institute of Aeronautics and Astronautics, 2006), p. 4845.

[13] K. Takahashi, K. Oguni, H. Yamada, and T. Fujiwara, Phys. Plasmas **15**, 084501 (2008).

[14] S. Shinohara and T. Soejima, Plasma Phys. Control. Fusion **40**, 2081 (1998).

[15] O. Grulke, A. Stark, T. Windisch, J. Zalach, and T.Klinger, Contrib. Plasma Phys. **47**, No. 3, 183 (2007).

[16] K. Takahashi, C. Charles, and R. W. Boswell, and R. Hatakeyama, Phys. Plasmas **15**, 074505 (2008).